CA3ViAR

Design of a composite UHBR fan

5th – 6th September 2022

Aerodynamic design of a scaled UHBR fan

Torben Eggers, Jens Friedrichs
Institute of Jet Propulsion and Turbomachinery
TU Braunschweig

Agenda

- Introduction
- Fan Stage Design Process
- Aerodynamic Design
- Conclusions and Outlook

Introduction

Design trend of future turbofan engines

- increasing bypass ratio to reduce specific fuel consumption
- shortened intake length to reduce the wetted intake surface

Aerodynamic and structural challenges

- reduced stall margin with increasing risk of fan flutter
- stronger coupling of rotor and intake can enlarge flutter bite
- slender and highly loaded blade structures

Goals of CA3ViAR

- design a scaled ultra-high bypass ratio (UHBR) fan with composite rotor blades, which features aeroelastic phenomena under certain operating points within the wind tunnel
- get a better understanding of phenomena and multi-physical effects at off-design
- provide an open test case

Fig.1: Modern turbofan engine - CFM International LEAP-1C [1]

Fan Stage Design Process

Specify top level fan design parameters

- trends in commercial a/c engine developement
- facility constraints (hub-to-tip ratio, max. rpm, etc.)
- rig compatibility with INFRa Project

Design targets

- values based on A320-Neo specifications
- cruise for engine design point
- take-off for rig investigations

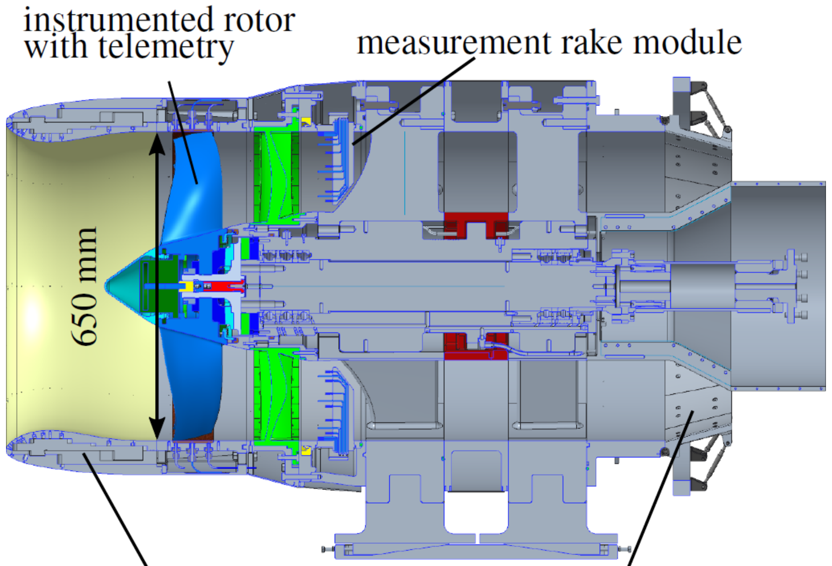

Fig.2: INFRa test rig

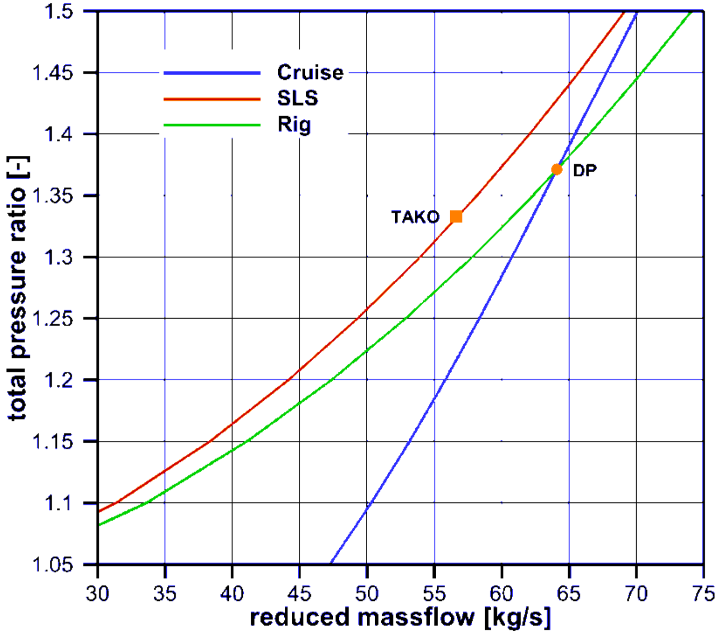

Fig.3: Definition of aerodynamic design point

Fan Stage Design Process

<u>Iterative design process</u>

- linked aerodynamic and aeroelastic tool chain
- design constrained by existing rig

<u>Approach</u>

- engine cycle design of a modern UHBR-turbofan using GasTurb
- scaling for rig dimensions based on Mach number similarity
- meridional design for annulus dimensions and radial flow distribution
- blade aerodynamic design using sub- and supersonic methods and aerodyn. load control factors (DF, DH, etc.)
- high fidelity 3D-RANS-CFD analysis for design and off-design operating points (Take-Off & Approach)

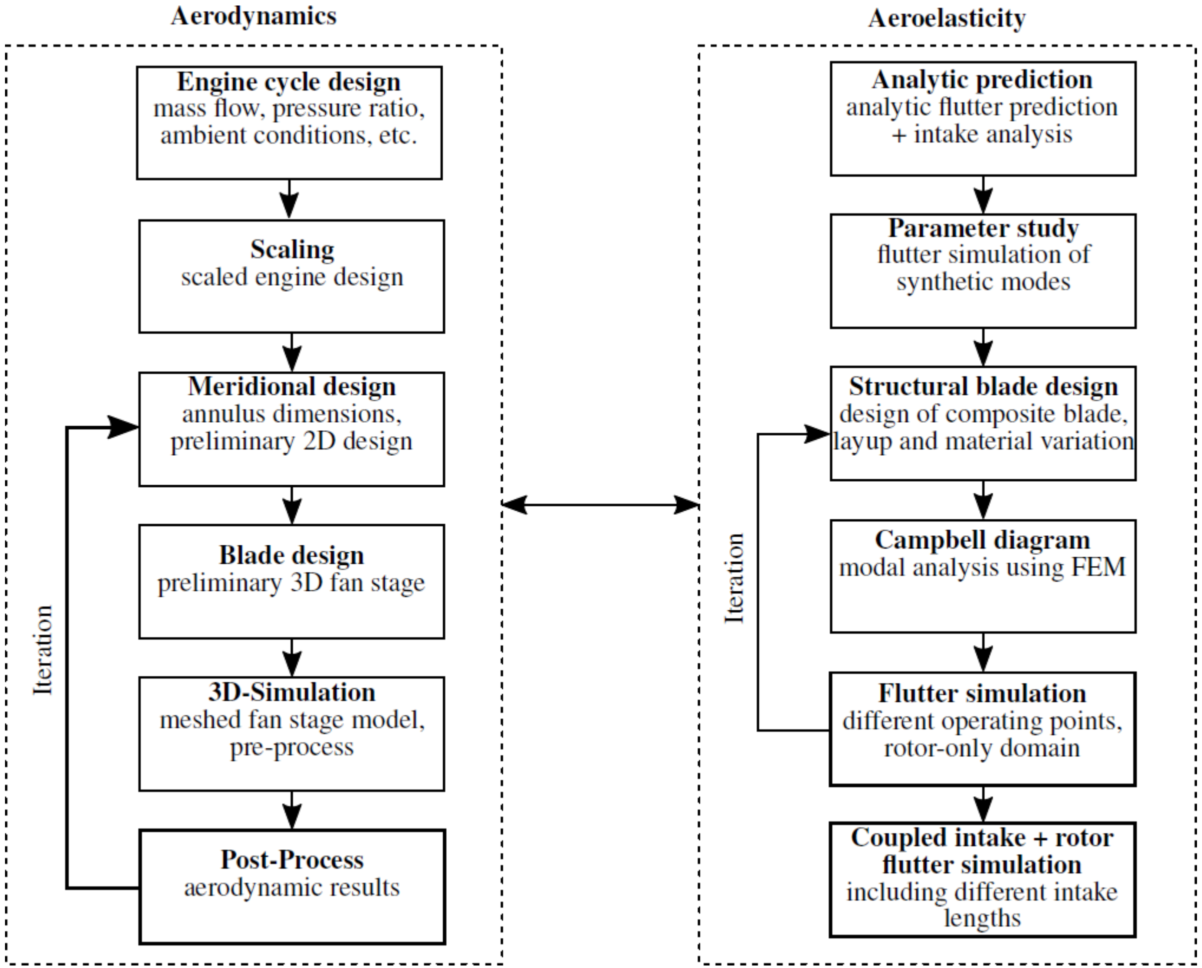

Fig.4: Design process

Aerodynamic Design

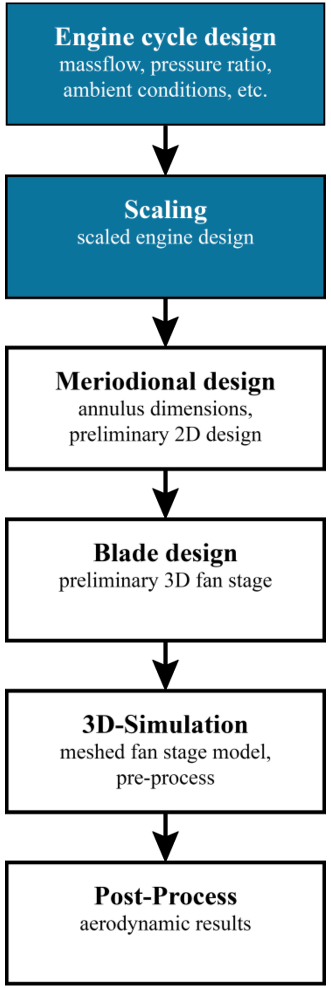

Engine cycle design & scaling

- cycle design based on literature values for an UHBR geared turbofan using GasTurb 13
- cruise condition as reference design point
- take-off as reference rig operation point
- constraints in max. speed, tip radius and pressure ratio
- geometrical similarity met at approximately 1:3.3
- Mach similarity met

Tab.1: Design parameters

Parameters	Design (10.7km)	Rig (0km)	
$Operation$	Cruise	Cruise	Take-Off
BPR	17	17	17
Ma_z	0.62	0.62	0.52
η_{poly}	0.89	0.89	0.89
π_t	1.37	1.37	1.32
$\dot{m}$ $(^{kg}/_{s})$	272.24	63.39	57.15
n_{Fan} $(^{1}/_{min})$	2375	8667	8095
V_θ $(^{m}/_{s})$	272	295	275
r_{tip} (m)	1.093	0.325	0.325
ν	0.26	0.26	0.26

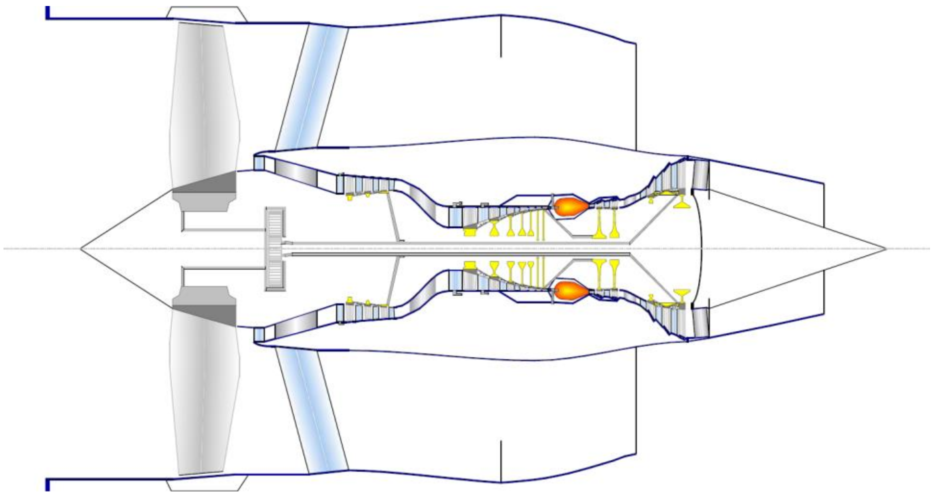

Fig.5: GasTurb design

Aerodynamic Design

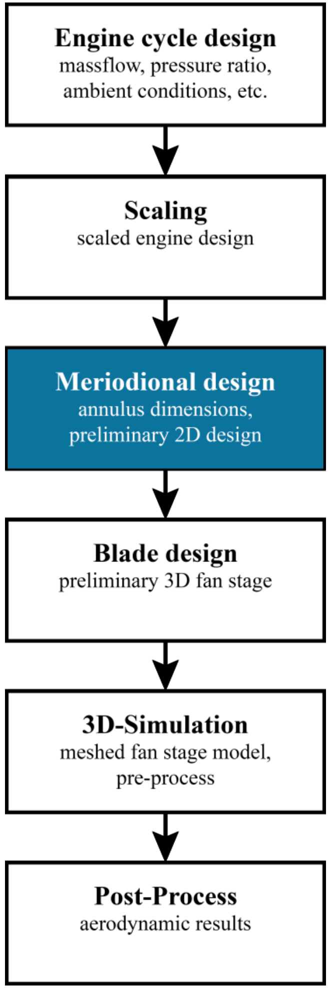

<u>Meridional design</u>

- hub and shroud contour taken from rig constraints
- ISRE design for radial distribution $V_z - V_{z,i} = 2c_p(T - T_i) - \left({V_\theta}^2 - {V_{\theta,i}}^2\right) - \int_{r_i}^{r} \frac{2{V_\theta}^2}{r} dr$
- vortex theory from NASA-SP36
- calculation of blade numbers based on aspect ratio (rotor) and cut-off frequency (stator)

Tab.2: Meridional design parameters

Design parameters	Design
Flow coefficient φ_{mean}	0.69
Work coefficient ψ_{mean}	1.59
Poly. efficiency η_{poly} [-]	0.86
Fan total pressure ratio π [-]	1.37
Rotor blades	18
Stator blades	40

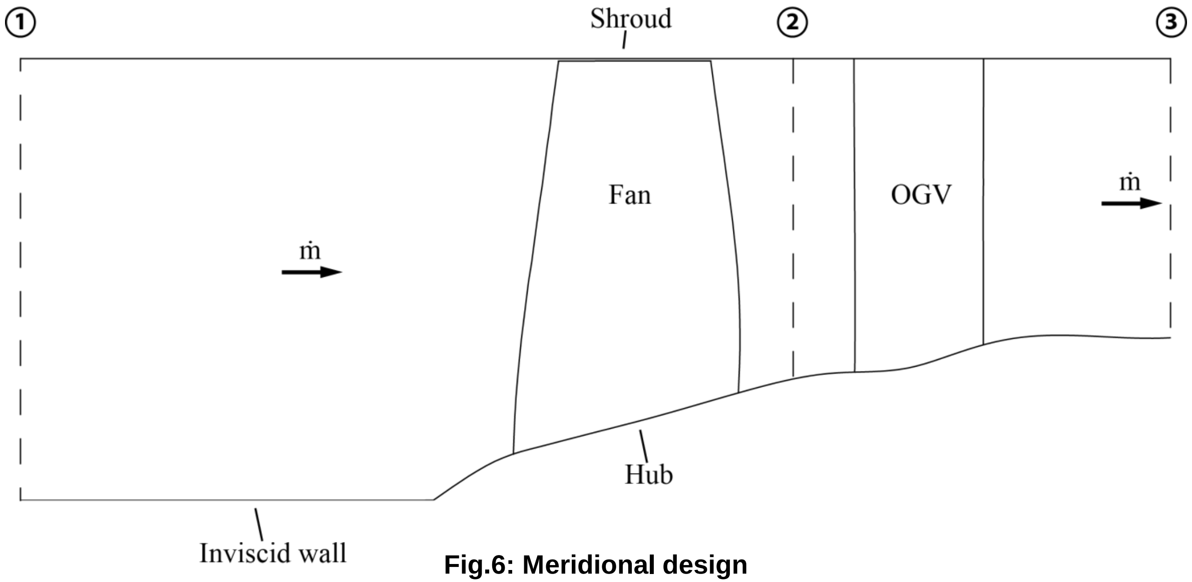

Fig.6: Meridional design

Aerodynamic Design

Engine cycle design
massflow, pressure ratio, ambient conditions, etc.

↓

Scaling
scaled engine design

↓

Meriodional design
annulus dimensions, preliminary 2D design

↓

Blade design
preliminary 3D fan stage

↓

3D-Simulation
meshed fan stage model, pre-process

↓

Post-Process
aerodynamic results

Blade design

- superposition of cubic thickness distribution and parabolic camber line
- elliptical leading and trailing edge
- staggering and threading at center of gravity
- tip clearance of 0.5 mm
- minimum manufacuturable thickness of 0.62 mm

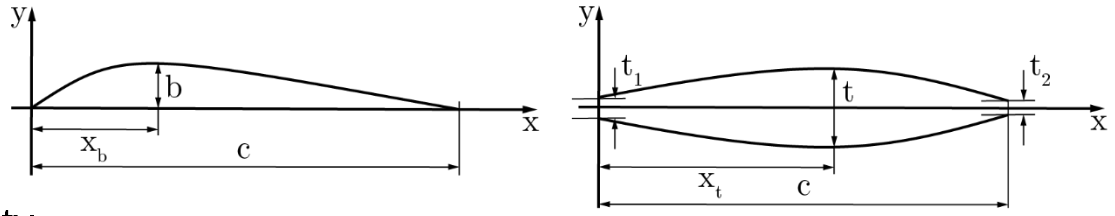

Fig.7: Parabolic camber line [2] (left) und thickness distribution [3] (right)

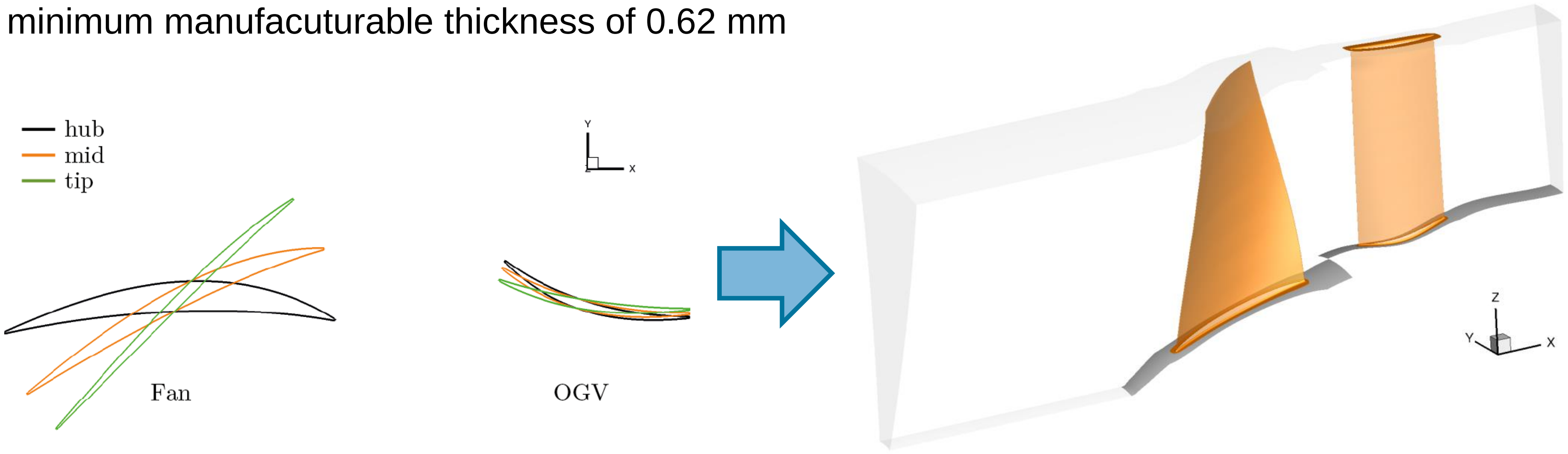

Fig.8: Profile sections and 3D blades

Aerodynamic Design

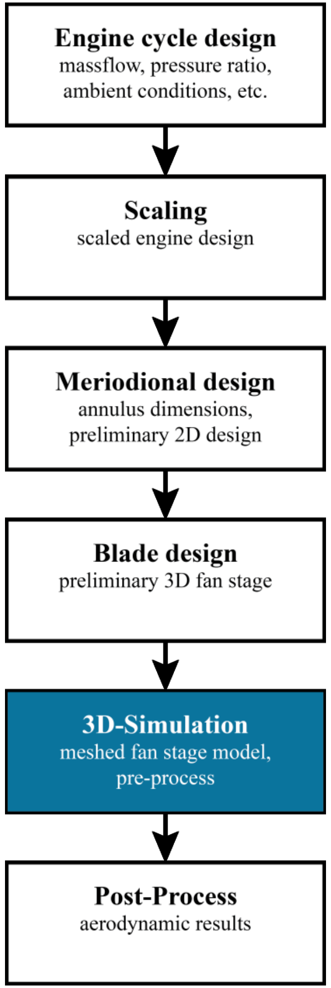

<u>Numerical setup</u>

- mesh generation with AutoGrid Numeca 12.2rc
- one pitch periodic domain of 4.1×10^6 cells
- resolution of boundary layer with $y^+ \approx 1$
- mesh independence proven with GCI of 0.01%
- simulations done with the 3D RANS solver TRACE Version 9.1.7

Tab.3: Setup parameters

Setting	Parameter
Mode	RANS
Wall treatment	Low-Reynolds
Inlet	$p_{t,1}, T_{t,1}, \beta_1, \beta'_1, l, I, Ma$
Outlet	p_3
Interface	Mixing Plane
Turbulence model	k-ω
Transition model	γ-Reθ

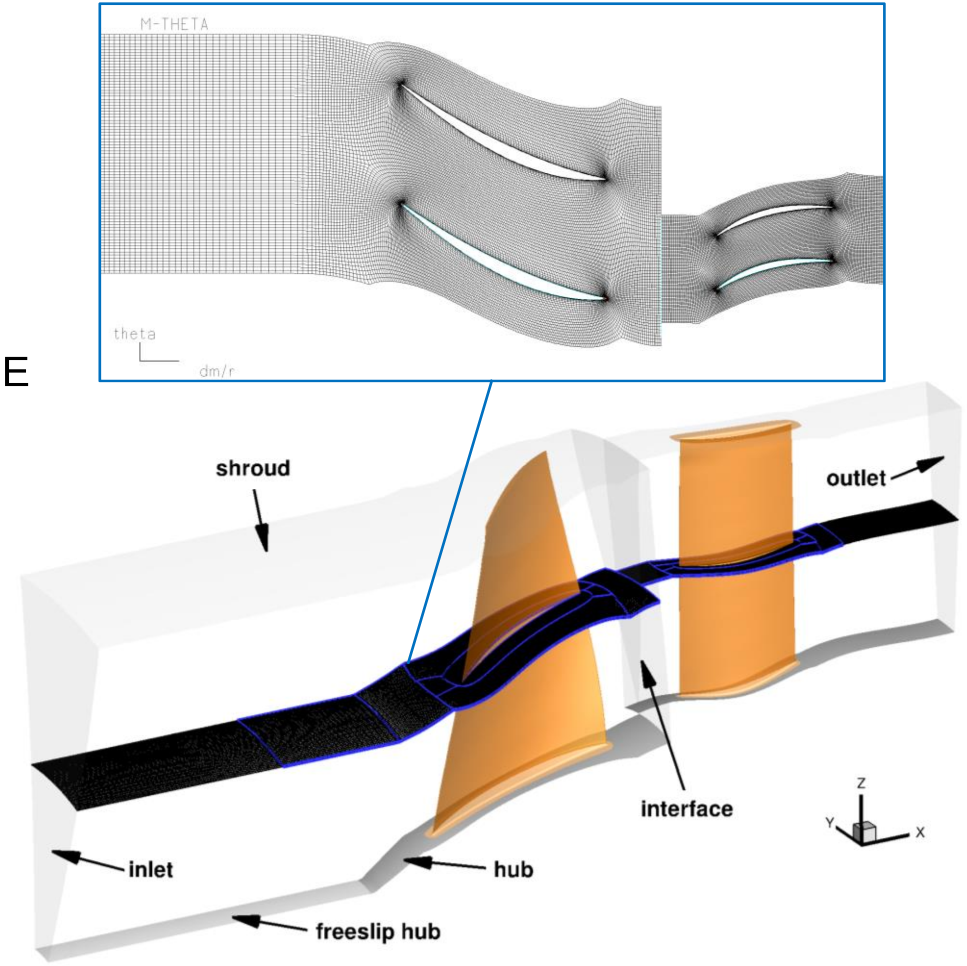

Fig.9: Numerical domain with mesh at 50% channel height

Aerodynamic Design

Engine cycle design
massflow, pressure ratio, ambient conditions, etc.

↓

Scaling
scaled engine design

↓

Meriodional design
annulus dimensions, preliminary 2D design

↓

Blade design
preliminary 3D fan stage

↓

3D-Simulation
meshed fan stage model, pre-process

↓

Post-Process
aerodynamic results

Aerodynamic fan characteristics

- simulation of speed lines
- post-processing of fan characteristics

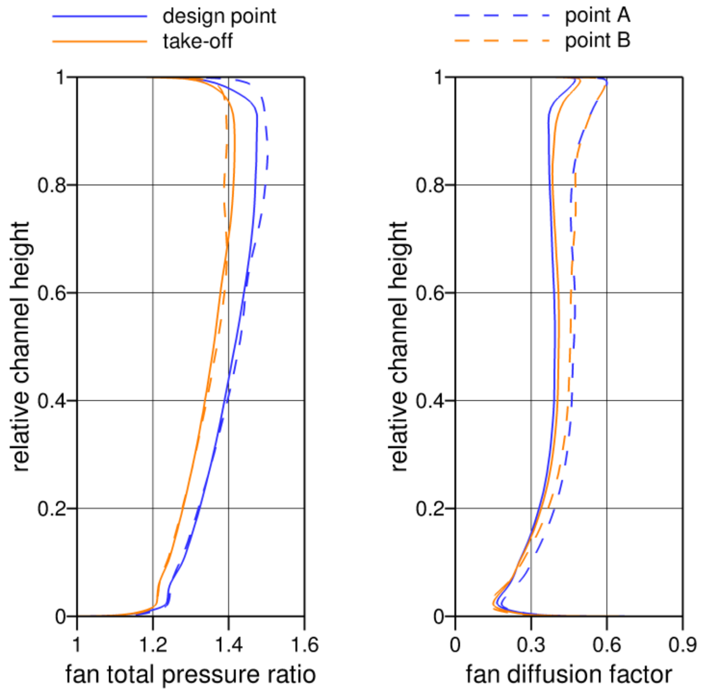

Fig.10: Radial distribution of fan characteristics

$$SM = 1 - \frac{\pi_{t,DP}}{\pi_{t,SL}} \frac{\dot{m}_{SL}}{\dot{m}_{DP}}$$

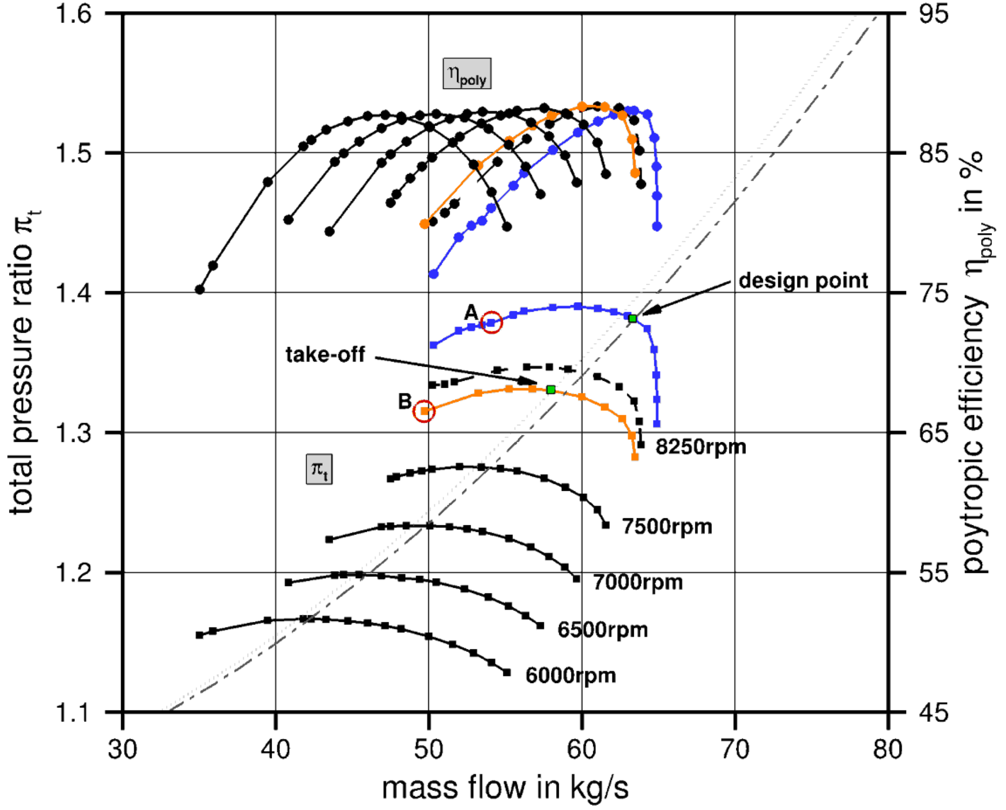

Fig.11: Fan performance map

Aerodynamic Design

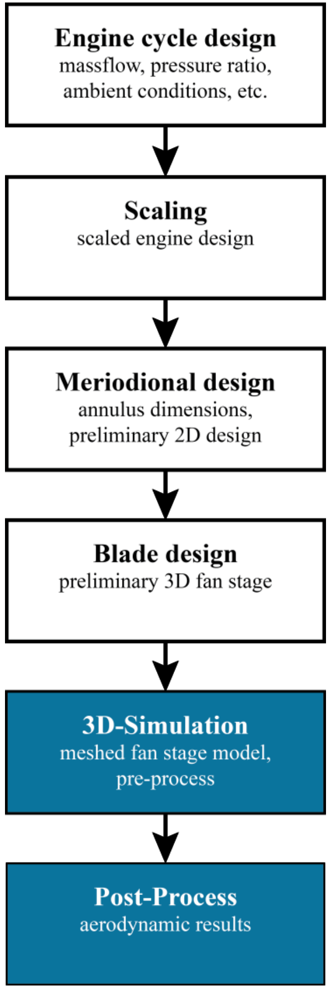

Tip gap sensitivity

- investigation of tip gap sensitivity to predict influence of blade elongation
- throttle lines for 0.5mm, 0.75mm and 1mm tip gap size
- study at design speed (8667rpm) and take-off (8095rpm)

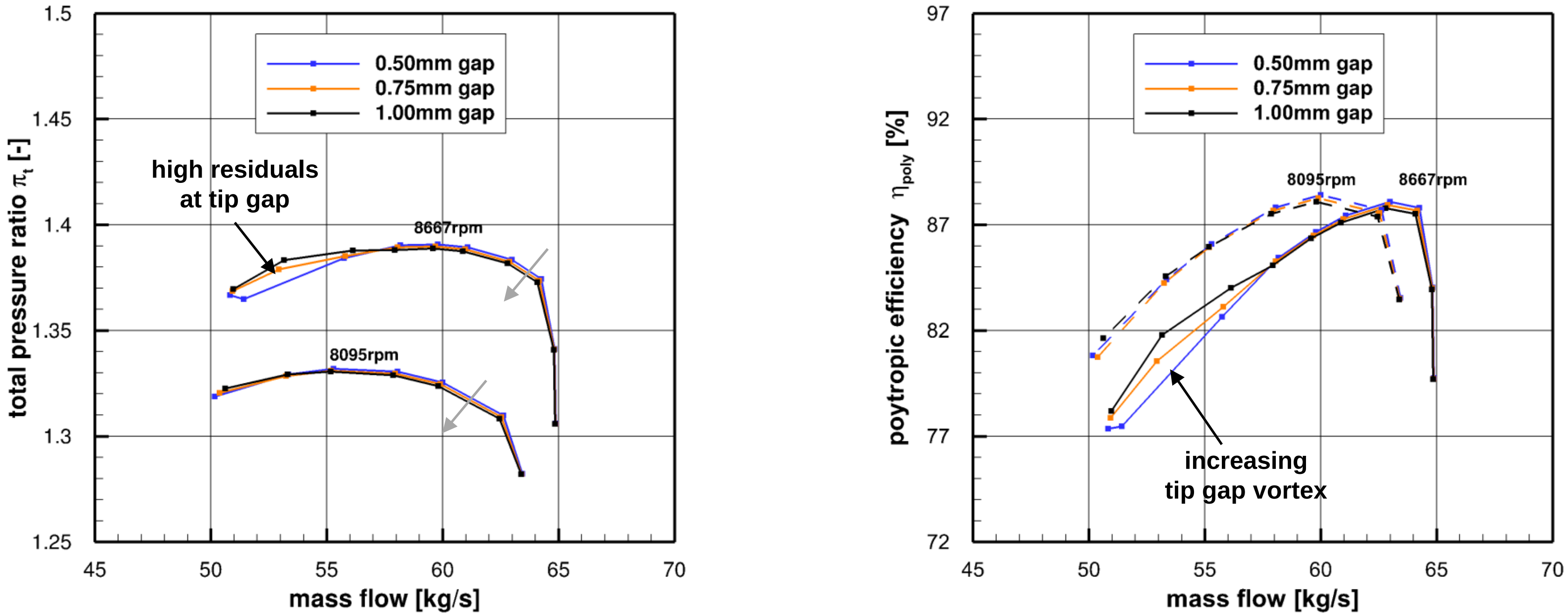

Fig.12: Influence of increasing tip gap size on the fan performance

Aerodynamic Design

Engine cycle design
massflow, pressure ratio, ambient conditions, etc.

↓

Scaling
scaled engine design

↓

Meriodional design
annulus dimensions, preliminary 2D design

↓

Blade design
preliminary 3D fan stage

↓

3D-Simulation
meshed fan stage model, pre-process

↓

Post-Process
aerodynamic results

Tip gap sensitivity

- total pressure ratio and polytropic efficiency drop linearly with increasing tip gap size
- target surge margin $SM_{cruise} \geq 11\%$ assured for all investigated tip gap sizes
- Increase in tip gap of 1% ~ -1.5% efficiency
- same behavior at take-off and cruise speed

Tab.4: Effect of tip gap size on fan stage performance

8667rpm	Tip gap	$\overline{\Delta\pi_t}$	$\overline{\Delta\eta_{poly}}$
0.50 mm	0.23 %	-	-
0.75 mm	0.35%	-0.07%	-0.17%
1.00 mm	0.46 %	-0.13%	-0.34%
8095 rpm	**Tip gap**	$\overline{\Delta\pi_t}$	$\overline{\Delta\eta_{poly}}$
0.50 mm	0.23 %	-	-
0.75 mm	0.35%	-0.06%	-0.18%
1.00 mm	0.46 %	-0.12%	-0.33%

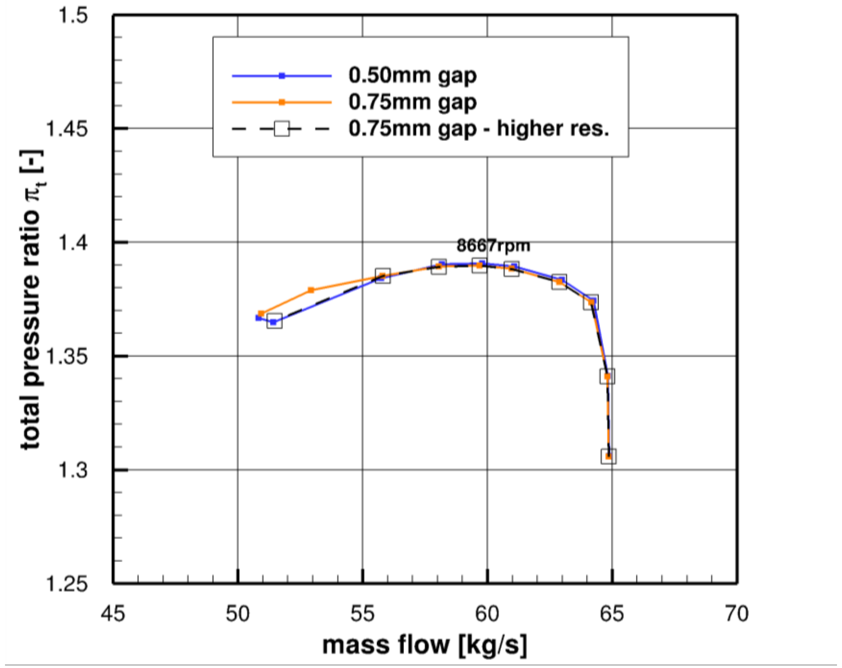

Fig.13: Effect of tip gap resolution on fan stage

Aerodynamic Design

Engine cycle design
massflow, pressure ratio, ambient conditions, etc.

↓

Scaling
scaled engine design

↓

Meriodional design
annulus dimensions, preliminary 2D design

↓

Blade design
preliminary 3D fan stage

↓

3D-Simulation
meshed fan stage model, pre-process

↓

Post-Process
aerodynamic results

Stall behavior of the fan stage

- total pressure ratio changes slightly with reducing mass flow for design speed
- significant total pressure drop at take-off speed

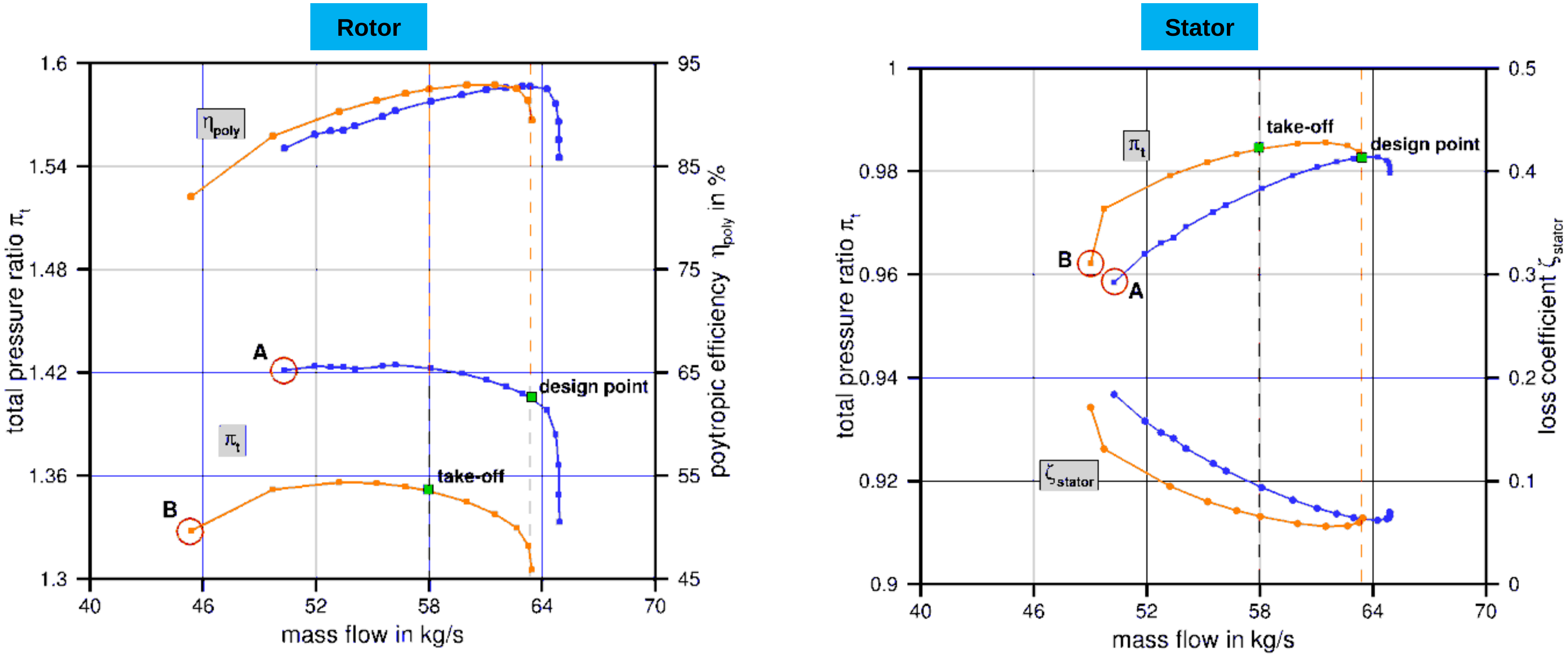

Fig.14: Part load behavior of fan stage rows

Aerodynamic Design

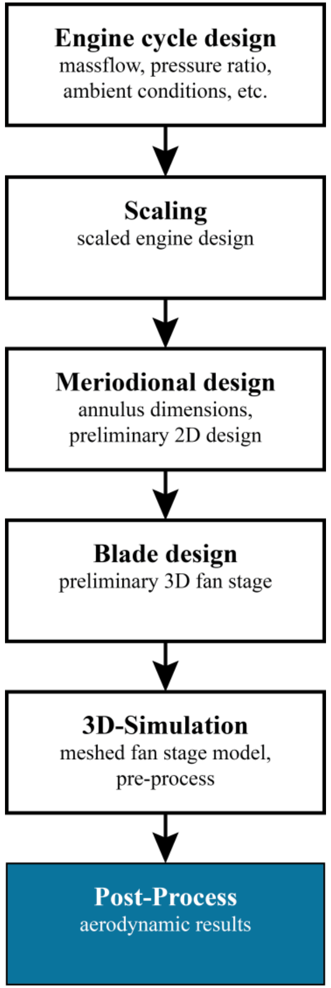

<u>Stall behavior of the fan stage</u>

- increasing incidence due to part load
- separations on rotor suction side at leading edge
- stator loss increases continuously, mainly due to interaction with tip gap vortex
- rotor driven stall behaviour is beneficial to flutter

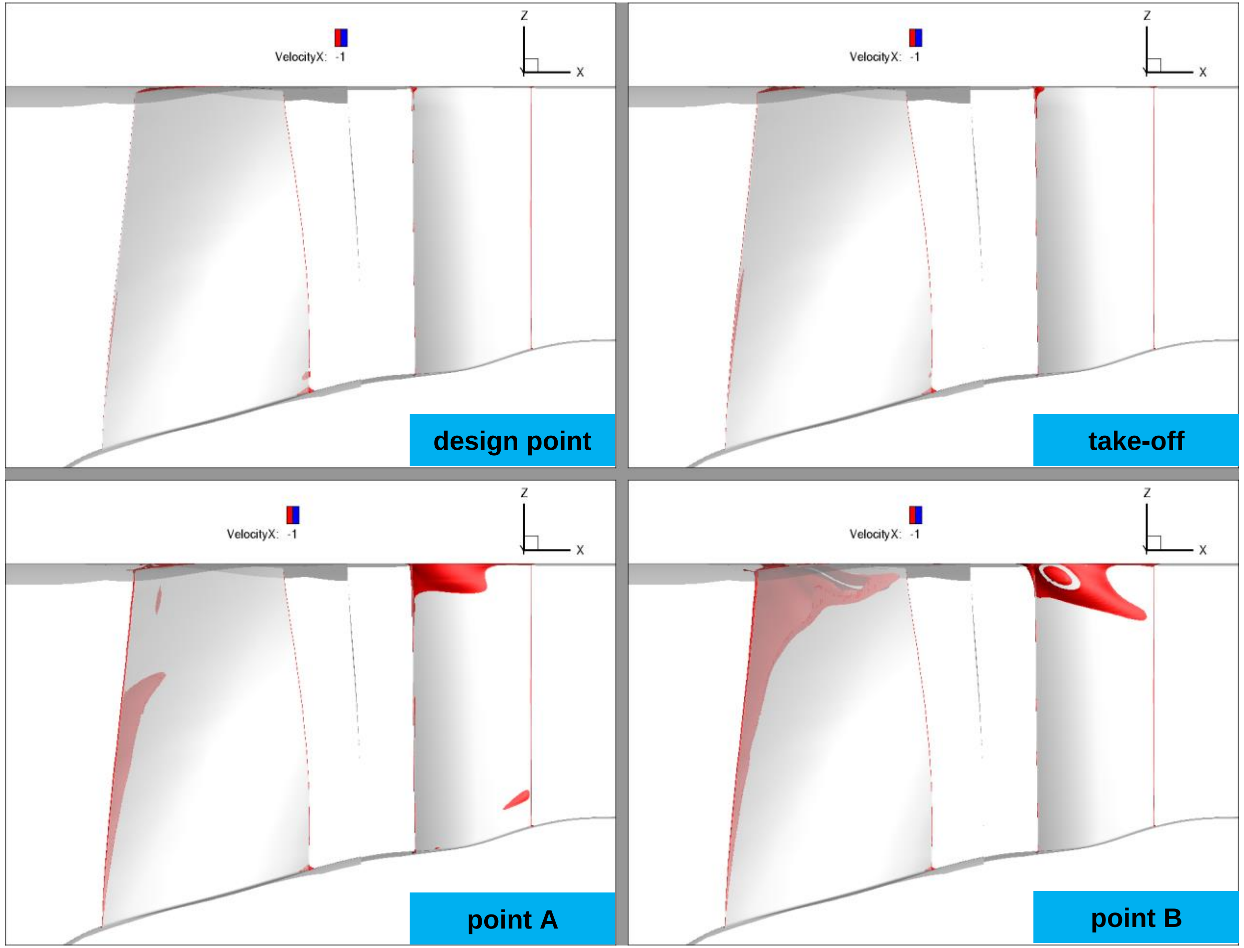

Fig.15: Iso-surfaces of flow separations

Technische Universität Braunschweig

IFAS Institut für Flugantriebe und Strömungsmaschinen

Aerodynamic Design

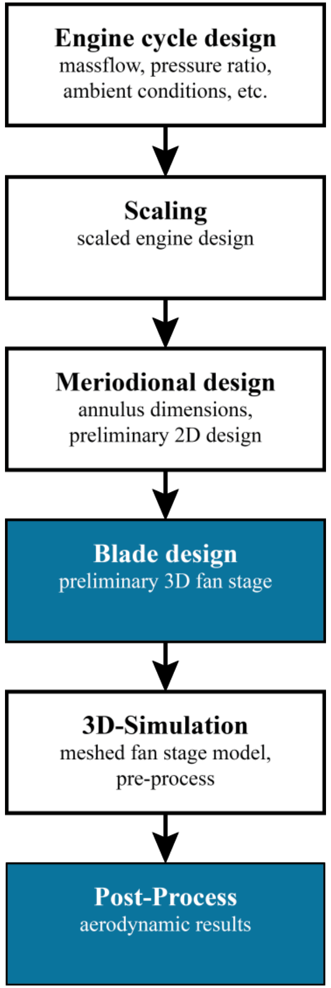

<u>Thickness reduction and camber adaption</u>

- reduction based on structural design and aeroelastic behavior
- thickness of rotor blade reduced to 75%
- increase of total pressure ratio and efficiency

Tab.5: Influence of fan blade thickness

	$\dot{m}$ [$^{kg}/_{s}$]	π [-]	η_{poly} [%]
Design target	63.4	1.37	89.2
Reference	63.4	1.37	87.6
Thin blade	63.4	1.37	87.6
Thin blade camber adap.	63.4	1.40	88.2

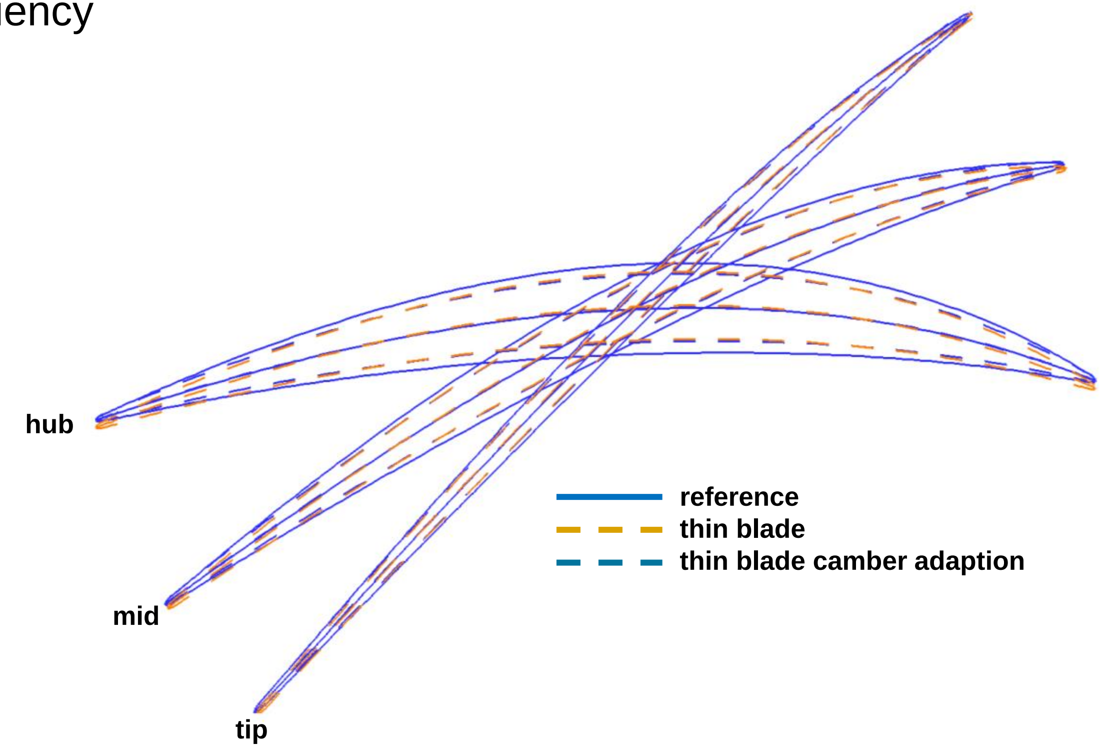

Fig.16: Fan profile sections

Aerodynamic Design

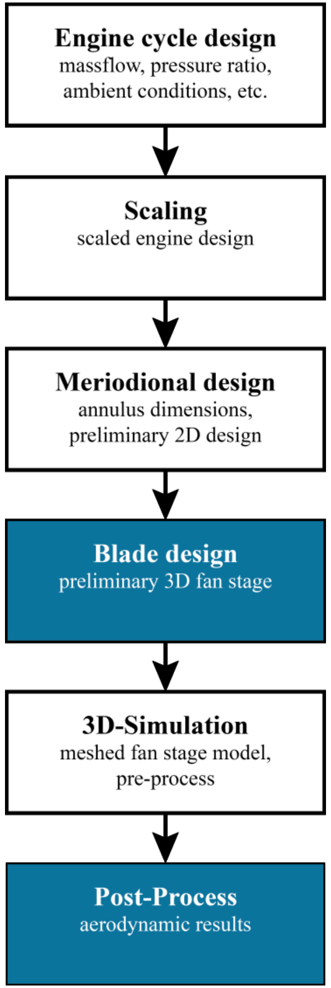

Thickness reduction and camber adaption

- flow gets redistributed due to larger hub passage
- turning and total pressure ratio of the fan is increased
- fan efficiency increased over 80% of relative channel height

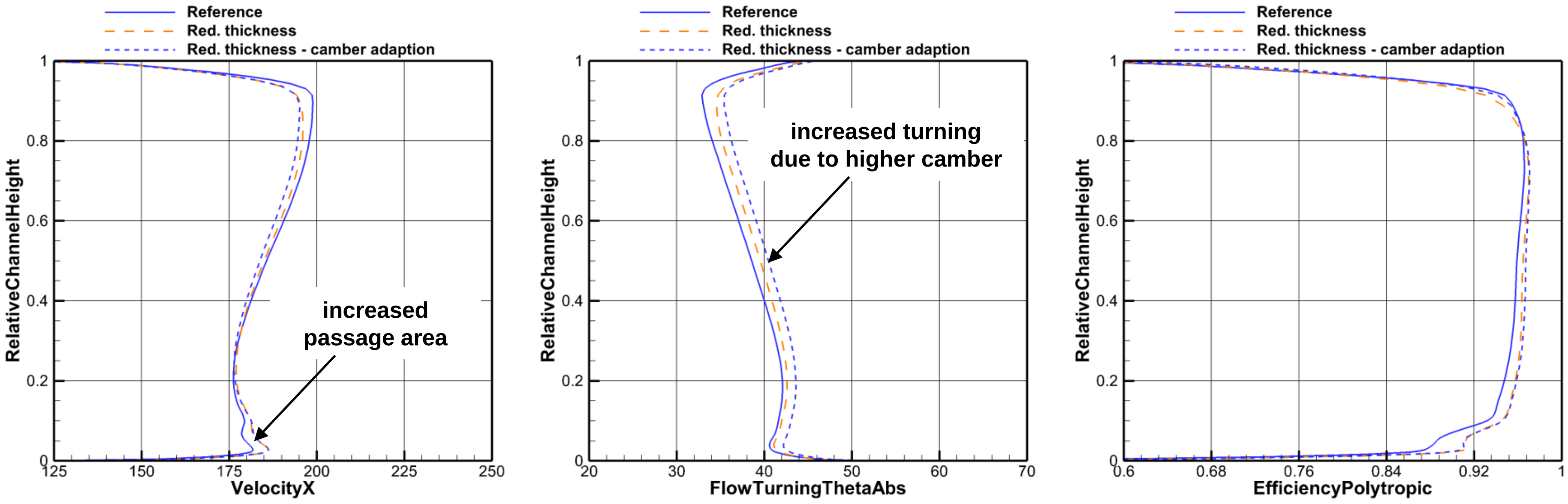

Fig.17: Effect of reduced blade thickness on radial distributions

Aerodynamic Design

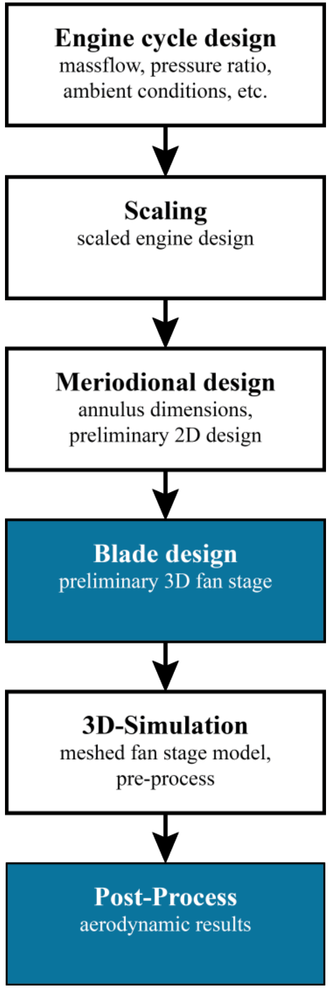

<u>3D blade design – sensitivity study</u>

- Fan cold shape shows elongation at trailing edge
- Behaviour not acceptable and requires a redesign
  1. Adaption of **maximum thickness position** in hub region (linear distribution: 0.35 – 0.65; before: 0.55 – 0.65)
  2. **Sweep** angle at tip ±10°
  3. **Lean** angle at tip ±10°
- Perform sensitivity study to examine the fan blade behaviour

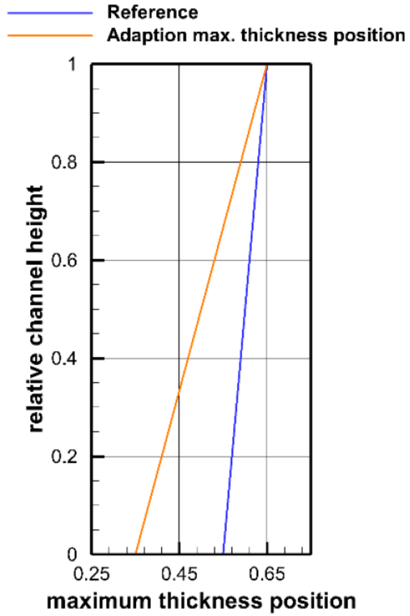

Fig.18: Adaption of max. thickness position

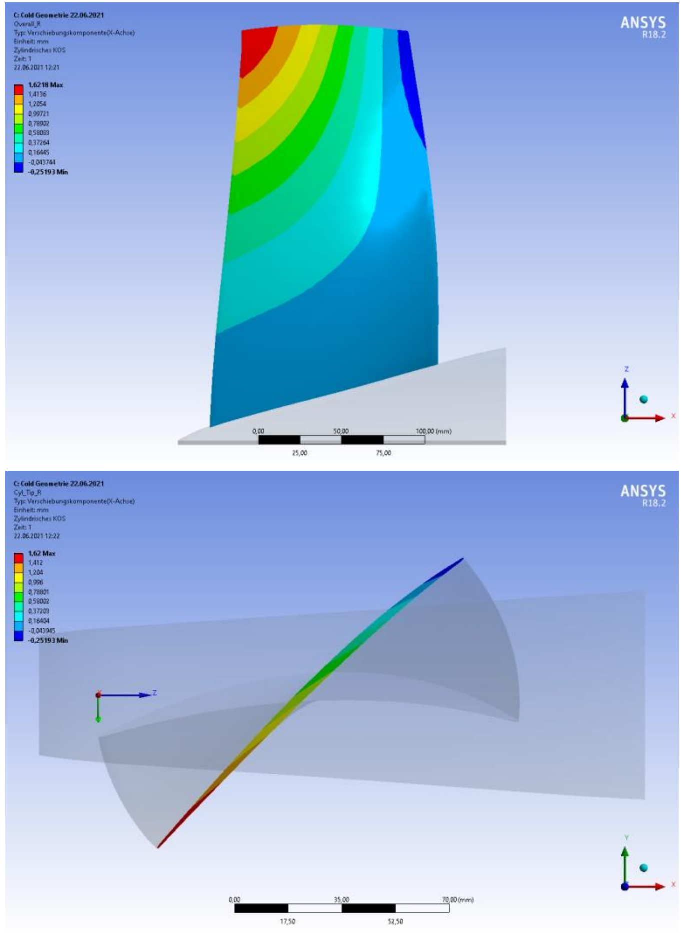

Fig.19: Cold fan blade under rotational loads

Aerodynamic Design

Engine cycle design
massflow, pressure ratio, ambient conditions, etc.

↓

Scaling
scaled engine design

↓

Meriodional design
annulus dimensions, preliminary 2D design

↓

Blade design
preliminary 3D fan stage

↓

3D-Simulation
meshed fan stage model, pre-process

↓

Post-Process
aerodynamic results

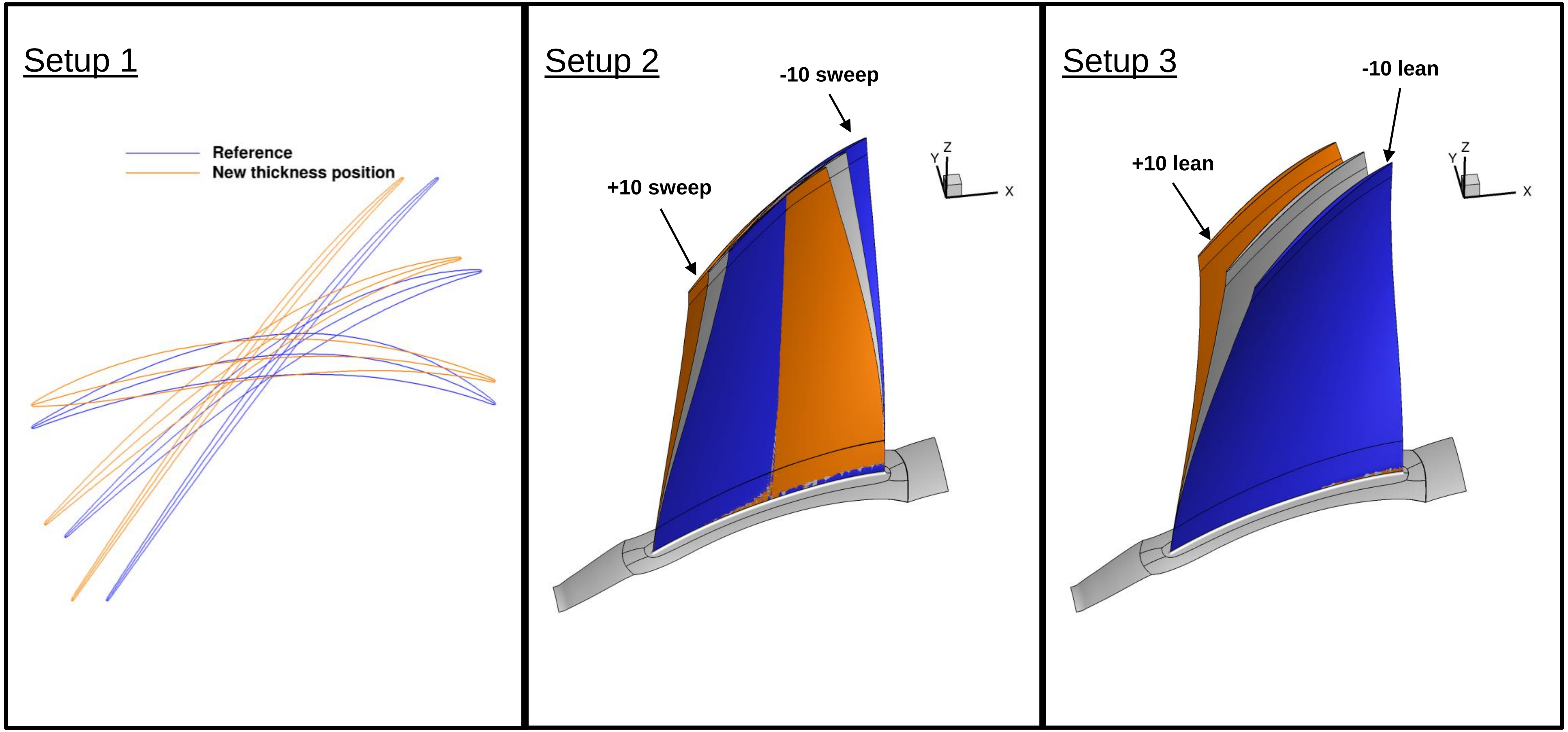

Fig.20: Fan redesign sensitivity setups

Aerodynamic Design

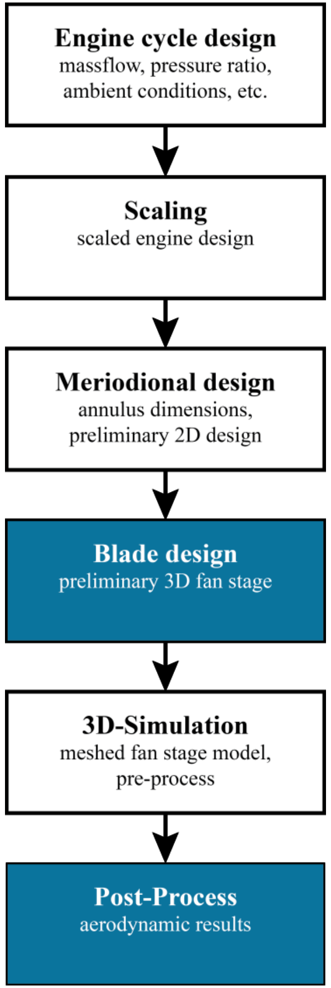

3D blade design – sensitivity study

- only positive sweep increases total pressure ratio and efficiency of the fan stage
- moving thickness upwards leads to a decreased flow turning and total pressure ratio
- all configuraions fullfil design criteria

Tab.6: Influence of 3D fan blade design

8667rpm (DP)	$\Delta\dot{m}$	$\overline{\Delta\pi_t}$	$\overline{\Delta\eta_{poly}}$
Reference	**63.4 kg/s**	**1.402**	**88.23 %**
Thickness position	-	-0.85 %	-0.46 %P
Sweep +10°	-	-0.00 %	+0.21 %P
Sweep -10°	-	-0.00 %	-0.15 %P
Lean +10°	-	+0.57 %	-0.05 %P
Lean -10°	-	-0.64 %	-0.02 %P

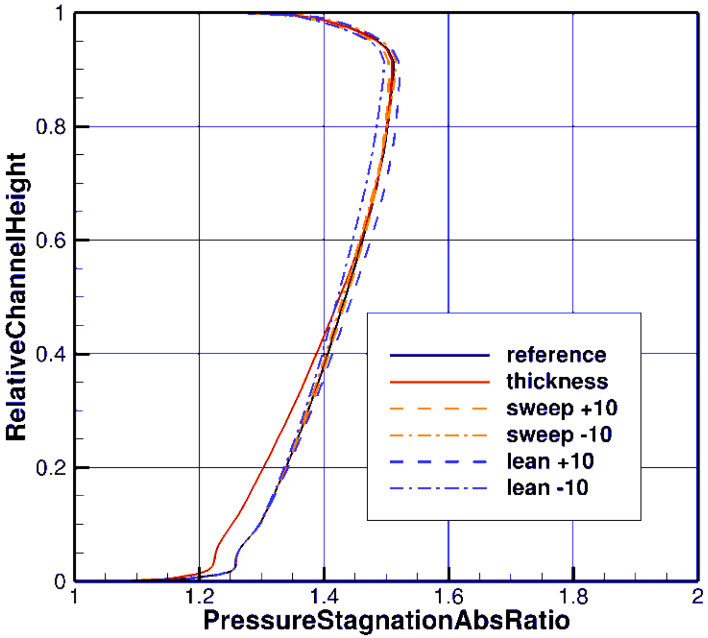

Fig.21: Radial distributions fan characteristics

Aerodynamic Design

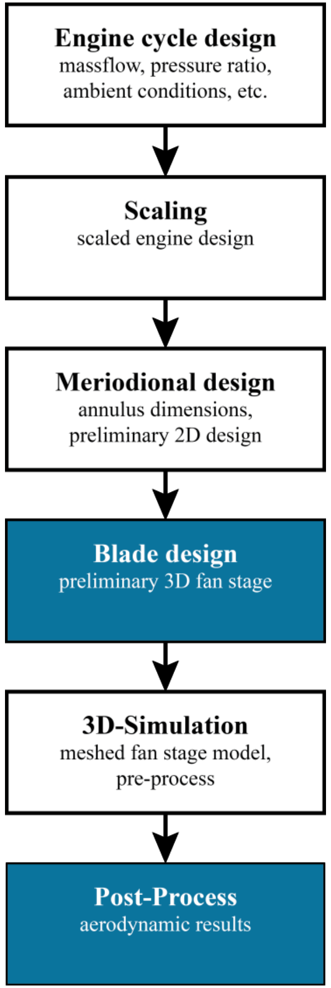

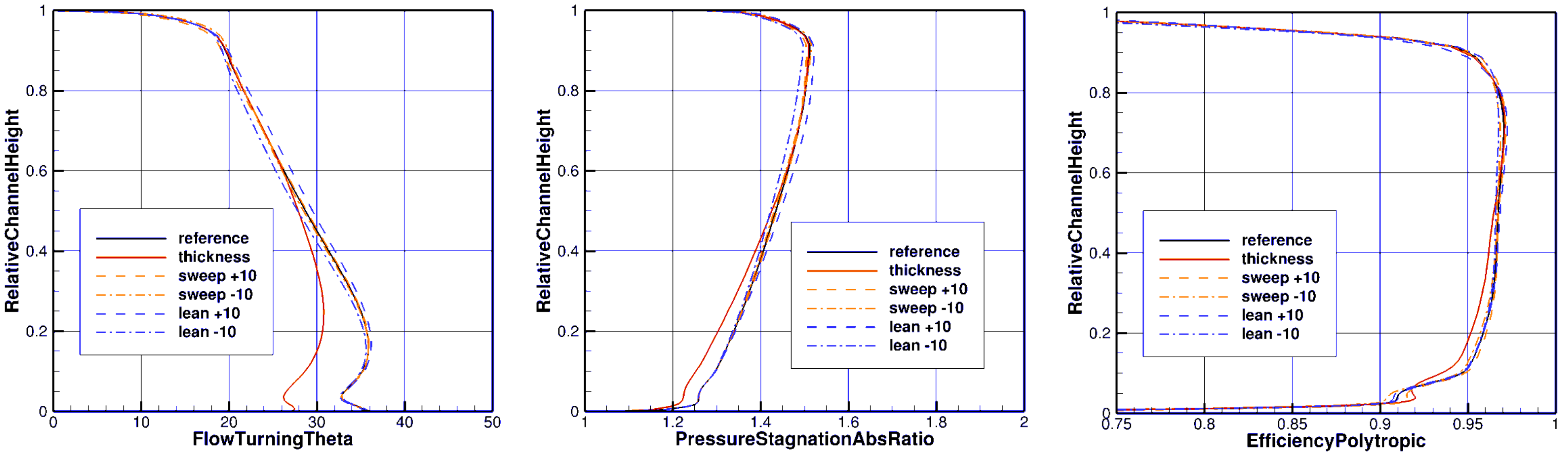

Fig.22: Radial distributions fan characteristics

Aeroelastic and structural feedback

- Positive lean affects the fan blade in the desired way
- Positive lean of +10° is too much and would reduce efficiency unnecessarily
- Adaption of thickness position is benefical for structural design, due to the reduced camber at the hub

Aerodynamic Design

Engine cycle design
massflow, pressure ratio, ambient conditions, etc.

↓

Scaling
scaled engine design

↓

Meriodional design
annulus dimensions, preliminary 2D design

↓

Blade design
preliminary 3D fan stage

↓

3D-Simulation
meshed fan stage model, pre-process

↓

Post-Process
aerodynamic results

Case173

- Positive lean 8° and reposition of max. thickness
- Positive radial displacement under load → problem solved ✓
- Reduced margin in negative damping ✘

Case175

- Positive lean 8° and reduced camber at the hub area
- Lean is added to adapt the elongation behaviour under loads
- Camber is reduced due to constructional constraints
- Reference maximum thickness position for negative damping
- Position of stacking line shifting downstream as the center of gravity moves downstream
- Positive radial displacement under loads ✓
- Sufficient negative damping ✓

Tab.7: 3D fan blade redesign

8667rpm (DP)	$\Delta\dot{m}$	$\Delta\overline{\pi_t}$	$\Delta\overline{\eta_{poly}}$
Reference	**63.4 kg/s**	**1.402**	**88.23 %**
Case173	-	-0.43 %	-0.6 %P
Case175	-	-0.93 %	-0.9 %P

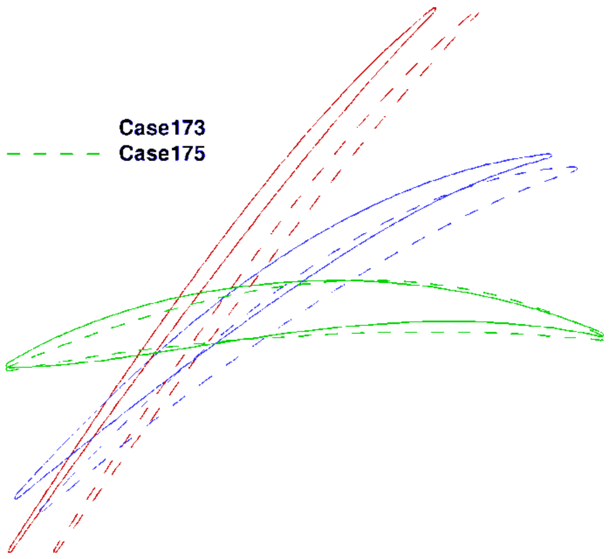

Fig.23: Fan blade sections for hub, mid & top

Aerodynamic Design

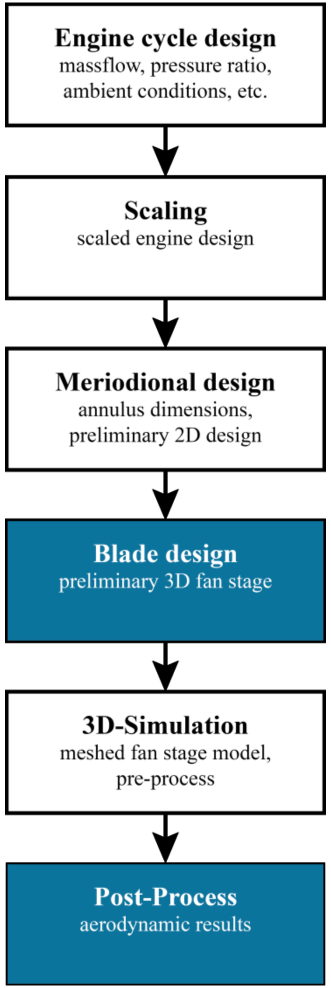

Tab.8: Final design

	$\dot{m}$ [$^{kg}/_{s}$]	π_t [-]	η_{poly} [%]
Design target	63.39 kg/s	1.37	89.2%
Case 175	63.39 kg/s	1.38 (+0.7%)	87.3% (-2.1%)

- Total pressure ratio target achieved
- Polytropic efficiency reduced in trade off for desired aeroelastic behaviour
- $SM_{cruise} \geq 16.4\%$ and $SM_{takeoff} \geq 11.0\%$ (target: $SM \geq 11\%$)

Aerodynamic fan stage design completed!

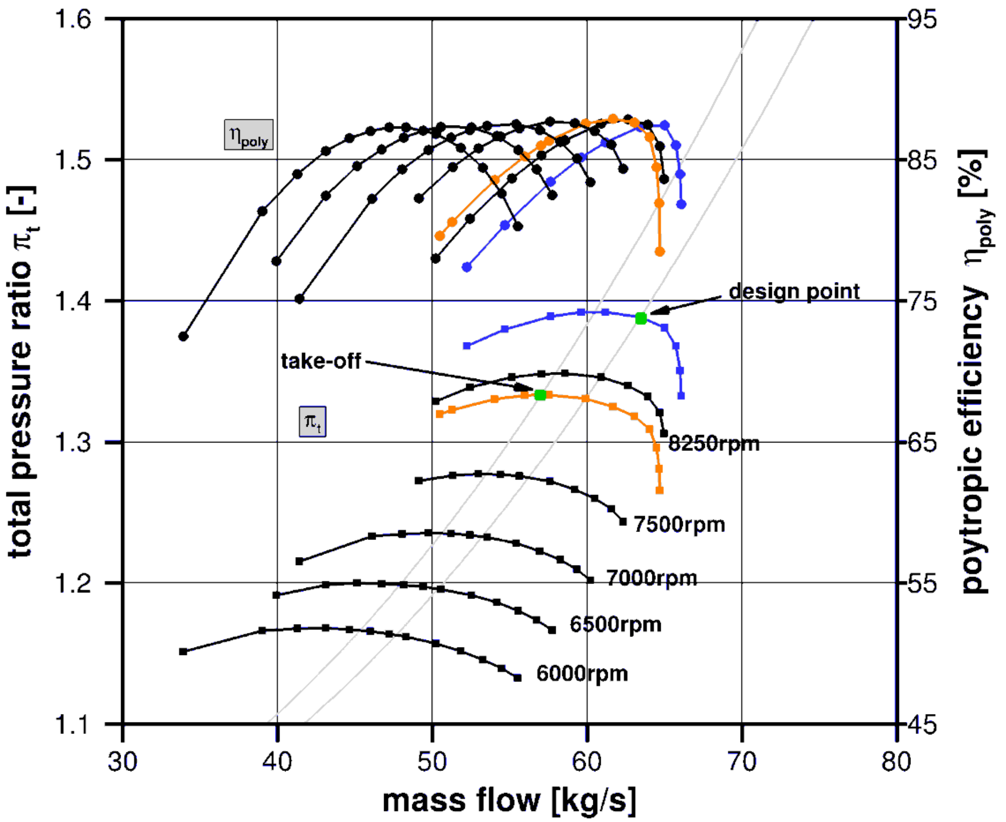

Fig.24: Speedlines calculations based on RANS simulations

Aerodynamic Design

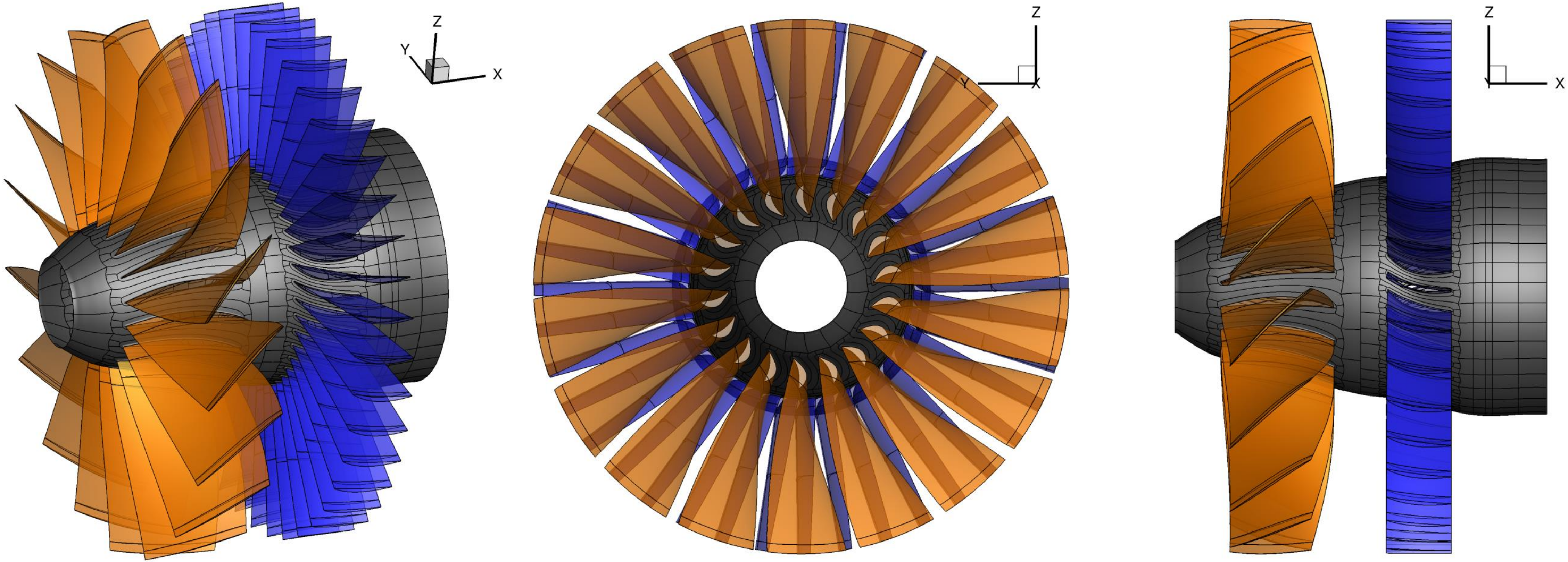

Fig.25: 3D model of final aerodynamic design

Conclusions and Outlook

Accomplishments

- design of a **fan stage** for a geared turbofan with a **bypass ratio of 17**
- sensitivity studies performed regarding **3D blade design** (sweep and lean)
- redesign of fan blade to **fulfill aeroelastic and structural** needs
- fan stage fulfills all design specifications and achieves a peak **polytropic efficiency of 87%**

Next steps

- **manufacturing** of the scaled UHBR fan stage
- further **post-test predictions** with additional **nacelle geometry**

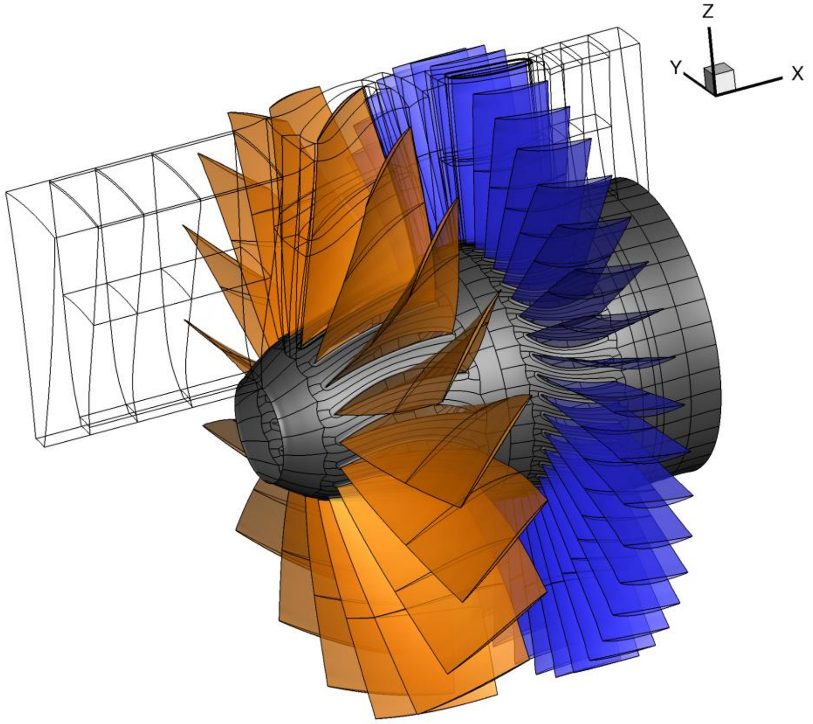

Fig.26: 3D fan model full annulus

Thank you for your attention

Acknowledgement:

This project has received funding from the Clean Sky 2 Joint Undertaking (JU) under grant agreement No 864256. The JU receives support from the European Union’s Horizon 2020 research and innovation programme and the Clean Sky 2 JU members other than the Union. This is gratefully acknowledge by the authors. Furthermore, the authors would like to acknowledge the German Aerospace Center (Deutsches Zentrum für Luft- und Raumfahrt, DLR) for providing TRACE.

References

[1] CFM International LEAP engine (2019). https://www.cfmaeroengines.com/engines/leap/

[2] Schlichting, H. ; Truckenbrodt, E. (2001): Aerodynamik des Flugzeuges. Erster Band: Grundlagen aus der Strömungstechnik Aerodynamik des Tragflügels (Teil I). 3. Auflage. Berlin, Heidelberg: Springer (Klassiker der Technik).

[3] Wennerstrom, A. J. (2000): Design of highly loaded axial-flow fans and compressors. White River Junction, Vt.: Concepts ETI.